Lanthanoid Rhenium Aluminides with a High Content of Aluminum: $LnRe_2Al_{10}$ (Ln = Ho−Lu) with a New Structure Type and $NdRe_2Al_{10}$ with $CaCr_2Al_{10}$-Type Structure

Birgit Fehrmann and Wolfgang Jeitschko*

Anorganisch-Chemisches Institut, Universität Münster, Wilhelm-Klemm-Strasse 8, D-48149 Münster, Germany

Received January 12, 1999

The title compounds were obtained by reaction of the elemental components with an excess of aluminum after dissolving the matrix in hydrochloric acid. The compounds $LnRe_2Al_{10}$ (Ln = Ho−Lu) crystallize with a new structure type, which was determined from single-crystal X-ray data of $LuRe_2Al_{10}$: *Cmcm*, $a = 929.1(1)$ pm, $b = 1027.7(2)$ pm, $c = 2684.1(5)$ pm, $Z = 12$. The two different lutetium atoms of the structure are coordinated by four rhenium and 16 aluminum atoms, while the two rhenium positions are in distorted icosahedral coordination of two lutetium and 10 aluminum atoms. The 12 different aluminum atoms have between 12 and 14 neighbors, of which two are rhenium and one or two are lutetium atoms. The structure may be considered as a stacking variant of the recently determined structure of $YbFe_2Al_{10}$. Both structures are related to that of $ThMn_{12}$. They contain hexagonally close-packed, puckered sheets similar to those known from the close-packed $TiAl_3$-type structure. In $LuRe_2Al_{10}$ and $YbFe_2Al_{10}$ these sheets of the compositions Re_2Al_6 and Fe_2Al_6, respectively, alternate with less densely packed layers of the composition $LnAl_4$. The crystal structures of $YbRe_2Al_{10}$ ($LuRe_2Al_{10}$ type, $a = 930.7(2)$ pm, $b = 1029.3(2)$ pm, $c = 2687.9(5)$ pm) and $NdRe_2Al_{10}$ ($CaCr_2Al_{10}$ type, $a = 1293.7(1)$ pm, $c = 517.4(1)$ pm) were also refined from single-crystal X-ray data. The refinements of the occupancy factors of these as well as those of 20 other intermetallic compounds with high aluminum content indicate a seemingly slightly lower (on average 2−3%) scattering power for the aluminum positions in all cases. This is ascribed to the differing electron distributions in the free and in the bonded aluminum atoms. The cell volume of $YbRe_2Al_{10}$ indicates a mixed or intermediate +II/+III valence of the ytterbium atoms.

Introduction

Many ternary lanthanoid transition metal aluminides with a high aluminum content are known, but just a few with rhenium as transition metal component. (We use the term "aluminides" for systematic reasons (sulfides, phosphides, silicides, aluminides) even though aluminum is usually not the most electronegative component of these compounds.) We have recently reported a series of hexagonal compounds $Ln_{7+x}Re_{12}Al_{61+y}$ with variable composition depending on the size of the rare earth metal atoms.[1,2] All other ternary lanthanoid rhenium aluminides with a high content of aluminum have crystal structures, which are related to the well-known tetragonal structure of $ThMn_{12}$. Of these the compounds $LnRe_4Al_8$ (Ln = Pr, Sm, Gd−Tm, Lu) have been known for some time.[3] They were found to be isotypic with $CeMn_4Al_8$, which represents an ordered substitution variant of the $ThMn_{12}$-type structure.[4]

The structure of the series $LnRe_2Al_{10}$ with the early light lanthanoids Ln = Ce, Pr, Sm[5] has been determined to be that of $CaCr_2Al_{10}$.[6] It has the same atomic positions as $ThMn_{12}$ with a $2^{1/2}$ times larger *a* axis due to the ordered distribution of chromium and aluminum atoms on the manganese position of $ThMn_{12}$. In aiming for isotypic new compounds with the heavy rare earth elements we found the series $LnRe_2Al_{10}$ (Ln = Ho−Lu), reported here. The structure of these compounds can be characterized as a stacking variant of the recently reported $YbFe_2Al_{10}$-type structure, which was described as a combined substitution and stacking variant of $ThMn_{12}$.[7] Numerous other ternary aluminides LnT_2Al_{10} (T = Fe, Ru, Os) with $YbFe_2Al_{10}$-type structure were reported recently.[8]

Sample Preparation, Properties, and Lattice Constants

The starting materials for the preparation of the new ternary compounds were the elemental components, all with nominal purities >99.9%. Filings of the rare earth elements were prepared under dry (Na) paraffin oil, which was removed with dry hexane. The filings of neodymium were stored under vacuum, and were only briefly exposed to air prior to the reactions. Aluminum was used in the form of turnings, which were obtained from ingots, and rhenium was purchased in the form of powder.

The compounds were synthesized by reaction of the elements with the atomic ratios Ln:Re:Al = 1:2:22 for the compounds $LnRe_2Al_{10}$ with Ln = Ho−Lu, and with the ratio 1:1:18 for the $CaCr_2Al_{10}$-type compound $NdRe_2Al_{10}$. The slightly compacted samples were placed in alumina crucibles, which in turn were sealed in silica tubes under argon and heated at a rate of 50

(1) Niemann, S.; Jeitschko, W. *J. Alloys Compd.* **1995**, *221*, 235.
(2) Thiede, V. M. T.; Gerdes, M. H.; Rodewald, U. Ch.; Jeitschko, W. *J. Alloys Compd.* **1997**, *261*, 54.
(3) Rykhal, R. M. *Vestn. L'vov. Politekh. Inst.* **1988**, *221*, 24; *Chem. Abstr.* **1989**, *111*, 121907v.
(4) Zarechnyuk, O. S.; Kripyakevich, P. I. *Kristallografiya* **1962**, *7*, 543.
(5) Thiede, V. M. T.; Jeitschko, W. *Z. Naturforsch.* **1998**, *53b*, 673.
(6) Cordier, G.; Czech, E.; Ochmann, H.; Schäfer, H. *J. Less-Common Met.* **1984**, *99*, 173.
(7) Niemann, S.; Jeitschko, W. *Z. Kristallogr.* **1995**, *210*, 338.
(8) Thiede, V. M. T.; Ebel, Th.; Jeitschko, W. *J. Mater. Chem.* **1998**, *8*, 125.

10.1021/ic990073n CCC: $18.00
Published on Web 06/24/1999

Table 1. Lattice Constants of the Compounds $LnRe_2Al_{10}$ Calculated from Guinier Powder Data[a]

compd	*a* (pm)	*b* (pm)	*c* (pm)	*V* (nm^3)
$CaCr_2Al_{10}$-type (Tetragonal)				
$NdRe_2Al_{10}$	1293.7(1)		517.4(1)	0.8660
$LuRe_2Al_{10}$-type (Orthorhombic)				
$HoRe_2Al_{10}$	930.2(2)	1030.5(2)	2692.1(4)	2.5805
$ErRe_2Al_{10}$	929.8(2)	1030.2(2)	2690.8(6)	2.5776
$TmRe_2Al_{10}$	930.5(1)	1028.7(2)	2686.5(5)	2.5714
$YbRe_2Al_{10}$	930.7(2)	1029.3(2)	2687.9(5)	2.5750
$LuRe_2Al_{10}$	929.1(1)	1027.7(2)	2684.1(5)	2.5630

[a] Standard deviations in the positions of the least significant digits are given in parentheses throughout the paper.

Table 2. Crystallographic Data for $LuRe_2Al_{10}$, $YbRe_2Al_{10}$, and $NdRe_2Al_{10}$[a]

empirical formula	$LuRe_2Al_{10}$	$YbRe_2Al_{10}$	$NdRe_2Al_{10}$
space group	*Cmcm* (No. 63)	*Cmcm* (No. 63)	*P4/nmm* (No. 129)
a (pm)	928.2(1)	929.4(2)	1294.3(2)
b (pm)	1027.2(2)	1029.8(2)	
c (pm)	2681.0(3)	2686.6(4)	517.12(7)
V (nm^3)	0.25562(6)	0.25713(8)	0.8665(2)
Z	12	12	4
fw	817.2	815.2	786.4
T (°C)	21	21	21
λ(pm)	71.07	71.07	71.07
ρ_{calcd} (g/cm^3)	6.37	6.31	6.03
μ (cm^{-1})	407	399	347
$R(F)^b$	0.0247	0.0456	0.0354
$R_w(F^2)^b$	0.0579	0.1524	0.0642

[a] The lattice constants were obtained on the four-circle diffractometer. [b] $R = \sum||F_o| - |F_c||/\sum|F_o|$; $R_w = |\sum w(F_o^2 - F_c^2)^2/\sum w(F_o^2)^2]^{1/2}$; $w = 1/[\sigma^2(F_o^2) + (VP)^2]$ where $P = (\mathrm{Max}(F_o^2) + 2F_c^2)/3$ and $V = 0.0128$ for $LuRe_2Al_{10}$, 0.0781 for $YbRe_2Al_{10}$, 0.0219 for $NdRe_2Al_{10}$.

°C/h to 850 °C, annealed at that temperature for 400 h, and subsequently cooled to room temperature at a rate of 6 °C/h. The aluminum-rich matrix was dissolved in diluted (0.05 N) hydrochloric acid, which attacks the ternary compounds at a much lower rate.

The compounds were obtained in the form of silvery shining, brittle crystals occasionally with the shape of square prisms. The powders are dark gray. They are stable in air for long periods of time. Energy-dispersive X-ray fluorescence analyses in a scanning electron microscope showed no impurity elements heavier than sodium.

All samples were characterized by their Guinier powder patterns using Cu Kα_1 radiation and α-quartz ($a = 491.30$ pm, $c = 540.46$ pm) as an internal standard. The lattice constants (Table 1) were refined by least-squares fits.

Structure Determination of $LuRe_2Al_{10}$

A single crystal of the lutetium compound was used for the structure determination of the isotypic aluminides $LnRe_2Al_{10}$ (Ln = Ho−Lu). X-ray data were recorded on an automated four-circle diffractometer (Enraf-Nonius CAD4) with $\theta/2\theta$ scans using graphite-monochromated Mo Kα radiation and a scintillation counter with pulse-height discrimination. Background counts were recorded at both ends of each scan. An empirical absorption correction was applied from ψ scan data. Additional details of the data collection are listed in Table 2 and in the Supporting Information.

The reciprocal lattice revealed orthorhombic symmetry, and the systematic extinctions led to the space groups *Cmcm*, *Cmc*2_1, and *C*2*cm* (a nonstandard setting of *Ama*2). The structure was successfully refined in the space group with the highest symmetry, the centrosymmetric group *Cmcm* (No. 63), using the program package SHELX-97.[9] The positions of the heavy atoms were deduced from a Patterson synthesis, and the aluminum atoms were located by difference Fourier analyses. For the refinement, a full-matrix least-squares program was used with atomic scattering factors which had been corrected for anomalous dispersion as provided by the program.[9] The weighting scheme reflected the counting statistics, and a parameter correcting for isotropic secondary extinction was optimized as a least-squares variable. As a check for the composition we also refined occupancy parameters for all atomic positions together with the thermal parameters, with the exception of the occupancy parameter of the 16-fold Re(1) position, which was held constant to fix the scale factor. The occupancy parameters varied between 96(1)% and 103(2)% (Table 3). Hence, no significant deviations from the full occupancies were found, and in the final refine-

Table 3. Atomic Parameters of $LuRe_2Al_{10}$, $YbRe_2Al_{10}$, and $NdRe_2Al_{10}$[a]

		occupancy	*x*	*y*	*z*	B_{eq}
$LuRe_2Al_{10}$ (Own Type, *Cmcm*)						
Lu(1)	8*f*	0.989(3)	0	0.12436(6)	0.08467(2)	0.75(1)
Lu(2)	4*c*	1.007(4)	0	0.38367(8)	1/4	0.56(2)
Re(1)	16*h*	1	0.25220(4)	0.00309(5)	0.16291(1)	0.286(6)
Re(2)	8*d*	1.001(2)	1/4	1/4	0	0.277(8)
Al(1)	16*h*	1.00(1)	0.2206(3)	0.2534(4)	0.1715(1)	0.61(4)
Al(2)	16*h*	1.00(2)	0.2477(4)	0.3716(3)	0.0832(1)	0.69(5)
Al(3)	16*h*	0.98(1)	0.3492(4)	0.1222(3)	0.0807(1)	0.69(5)
Al(4)	8*g*	0.97(2)	0.2925(5)	0.1105(4)	1/4	0.71(8)
Al(5)	8*g*	0.96(1)	0.3498(5)	0.3885(4)	1/4	0.68(7)
Al(6)	8*f*	0.99(2)	0	0.0943(4)	0.1994(2)	0.47(7)
Al(7)	8*f*	0.98(2)	0	0.1244(4)	0.6460(2)	0.76(7)
Al(8)	8*f*	0.99(2)	0	0.1645(4)	0.5340(2)	0.53(6)
Al(9)	8*f*	1.01(2)	0	0.3773(4)	0.0220(2)	0.58(7)
Al(10)	8*f*	0.97(2)	0	0.4019(4)	0.1345(2)	0.62(7)
Al(11)	8*f*	1.03(2)	0	0.6296(4)	0.1774(2)	0.72(7)
Al(12)	8*e*	1.01(2)	0.2058(4)	0	0	0.59(6)
$YbRe_2Al_{10}$ ($LuRe_2Al_{10}$-type, *Cmcm*)						
Yb(1)	8*f*	0.989(8)	0	0.1245(1)	0.08465(4)	0.99(2)
Yb(2)	4*c*	1.00(1)	0	0.3801(2)	1/4	0.91(3)
Re(1)	16*h*	1	0.25194(6)	0.0023(1)	0.16290(2)	0.68(2)
Re(2)	8*d*	1.000(6)	1/4	1/4	0	0.68(2)
Al(1)	16*h*	1.00(4)	0.2229(6)	0.2527(7)	0.1709(2)	0.83(7)
Al(2)	16*h*	0.93(4)	0.2485(5)	0.3717(6)	0.0831(2)	0.75(10)
Al(3)	16*h*	1.00(3)	0.3483(6)	0.1220(5)	0.0807(2)	1.14(9)
Al(4)	8*g*	0.96(5)	0.2888(9)	0.1105(8)	1/4	1.16(12)
Al(5)	8*g*	0.97(4)	0.3505(8)	0.3854(8)	1/4	1.17(12)
Al(6)	8*f*	0.90(4)	0	0.0903(8)	0.1997(3)	1.12(13)
Al(7)	8*f*	0.91(4)	0	0.1245(9)	0.6455(3)	1.45(13)
Al(8)	8*f*	0.96(4)	0	0.1661(8)	0.5335(3)	1.11(12)
Al(9)	8*f*	0.98(4)	0	0.3760(8)	0.0225(3)	1.21(13)
Al(10)	8*f*	0.94(4)	0	0.4028(8)	0.1339(3)	1.15(12)
Al(11)	8*f*	0.92(5)	0	0.6282(8)	0.1770(3)	1.40(13)
Al(12)	8*e*	1.11(5)	0.2086(9)	0	0	0.95(11)
$NdRe_2Al_{10}$ ($CaCr_2Al_{10}$-type, *P*4/*nmm*)						
Nd(1)	2*c*	0.988(6)	1/4	1/4	0.5149(2)	0.32(1)
Nd(2)	2*a*	0.984(6)	3/4	1/4	0	0.49(1)
Re	8*i*	1	1/4	0.50833(2)	0.2476(1)	0.250(6)
Al(1)	8*j*	0.94(2)	0.0749(1)	*x*	0.4737(6)	0.62(4)
Al(2)	8*j*	0.96(2)	0.1437(2)	*x*	0.0283(5)	0.59(4)
Al(3)	8*i*	1.14(2)	1/4	0.0110(2)	0.7486(8)	0.40(4)
Al(4)	8*h*	0.94(2)	0.3628(2)	$-x$	1/2	0.58(3)
Al(5)	8*g*	0.95(2)	0.4267(1)	$-x$	0	0.54(4)

[a] The structures were refined with ideal occupancies. The occupancy parameters listed in the third column were obtained from separate series of least-squares cycles. The last column contains the equivalent isotropic values B_{eq} of the anisotropic displacement parameters ($\times 10^{-4}$, pm^2), as defined by $B_{eq} = 8\pi^2 U_{eq}$, where U_{eq} is one-third of the orthogonalized $\mathbf{U}_{ij}$ tensor.

(9) Sheldrick, G. M. *SHELX-97: A Program Package for the Solution and Refinement of Crystal Structures*; Universität Göttingen: Göttingen, Germany, 1997.

Table 4. Interatomic Distances of $LnRe_2Al_{10}$ (Ln = Lu and Yb)[a]

		Ln = Lu/Yb			Ln = Lu/Yb			Ln = Lu/Yb			Ln = Lu/Yb
Ln(1):	1Al(7)	304.1/303.9	Al(1):	1Re(1)	258.9/258.9	Al(4):	2Re(1)	261.2/261.5	Al(8):	2Re(2)	264.6/264.1
	1Al(6)	309.5/311.1		1Re(1)	259.9/260.1		1Al(5)	263.7/265.4		1Al(9)	265.3/263.3
	1Al(9)	309.6/308.1		1Al(4)	265.3/265.4		2Al(1)	265.3/265.4		2Al(12)	271.0/273.9
	1Al(10)	315.1/315.6		1Al(2)	267.6/267.0		2Al(11)	274.9/278.5		2Al(2)	271.6/272.1
	1Al(8)	321.1/320.6		1Al(6)	272.6/277.4		1Al(5)	290.6/288.8		2Al(3)	288.9/289.1
	2Al(12)	323.3/325.4		1Al(10)	274.1/277.1		1Ln(2)	302.5/308.0		1Al(7)	303.5/303.9
	2Al(3)	324.6/324.4		1Al(5)	279.4/279.3		2Al(6)	304.2/301.6		1Ln(1)	321.1/320.6
	1Al(8)	326.6/329.1		1Al(11)	289.6/288.4		(1Al(4)	385.7/393.2)		1Ln(1)	326.6/329.1
	2Al(1)	337.5/337.9		1Al(7)	296.4/295.2		1Ln(2)	390.7/386.3		1Al(8)	384.1/386.5
	2Re(1)	338.4/339.2		1Al(3)	303.1/300.7	Al(5):	1Al(4)	263.7/265.4	Al(9):	1Al(8)	265.3/263.3
	2Al(2)	342.8/343.9		1Ln(2)	323.0/324.8		2Re(1)	278.4/279.9		2Re(2)	273.0/273.1
	2Re(2)	349.7/350.2		1Ln(1)	337.5/337.9		1Al(5)	279.0/278.3		1Al(9)	278.5/282.5
	2Al(2)	350.0/350.0	Al(2):	1Re(1)	253.1/253.2		2Al(1)	279.4/279.3		2Al(2)	282.8/282.9
Ln(2):	2Al(4)	302.5/308.0		1Re(2)	255.9/256.0		2Al(6)	287.5/286.7		1Al(10)	303.1/300.9
	2Al(10)	310.5/312.9		1Al(12)	263.0/262.5		1Al(4)	290.6/288.8		2Al(12)	306.8/305.8
	2Al(11)	319.2/322.1		1Al(1)	267.6/267.0		2Al(7)	312.3/313.7		2Al(3)	309.2/311.2
	4Al(1)	323.0/324.8		1Al(10)	270.1/270.5		1Ln(2)	325.1/326.2		1Ln(1)	309.6/308.1
	2Al(5)	325.1/326.3		1Al(8)	271.6/272.1		2Al(11)	358.2/357.8		2Al(3)	328.4/329.6
	2Al(6)	326.9/327.5		1Al(3)	272.9/273.0	Al(6):	1Al(7)	266.6/264.7	Al(10):	1Al(11)	260.6/259.2
	4Re(1)	350.3/352.1		1Al(3)	273.1/273.4		2Re(1)	270.7/270.1		2Re(1)	263.8/264.3
	2Al(4)	390.7/386.3		1Al(9)	282.8/282.9		1Al(6)	271.6/270.7		2Al(2)	270.1/270.5
Re(1):	1Al(2)	253.1/253.2		1Al(7)	288.8/288.0		2Al(1)	272.6/277.4		2Al(1)	274.1/277.1
	1Al(1)	258.9/258.8		1Ln(1)	342.8/343.9		2Al(5)	287.5/286.7		1Al(9)	303.1/300.9
	1Al(1)	259.9/260.1		1Ln(1)	350.0/350.0		2Al(4)	304.2/301.6		2Al(3)	302.9/302.1
	1Al(4)	261.2/261.5	Al(3):	1Re(1)	267.9/268.4		1Ln(1)	309.5/311.1		1Ln(2)	310.5/312.9
	1Al(10)	263.8/264.3		1Re(2)	269.6/269.8		1Ln(2)	326.9/327.5		1Ln(1)	315.1/315.6
	1Al(11)	267.2/267.4		1Al(2)	272.9/273.0		1Al(10)	360.9/367.0		1Al(6)	360.9/367.0
	1Al(3)	267.9/268.4		1Al(2)	273.1/273.4	Al(7):	1Al(11)	266.5/268.3	Al(11):	1Al(10)	260.6/259.2
	1Al(6)	270.7/270.1		1Al(3)	280.3/282.3		1Al(6)	266.6/264.7		1Al(7)	266.5/268.3
	1Al(7)	272.3/272.4		1Al(12)	283.6/282.4		2Re(1)	272.3/272.4		2Re(1)	267.2/267.4
	1Al(5)	278.4/279.9		1Al(8)	288.9/289.1		2Al(2)	288.8/288.0		2Al(4)	274.9/278.4
	1Ln(1)	338.4/339.2		1Al(11)	294.9/294.7		2Al(1)	296.4/295.2		2Al(1)	289.6/288.4
	1Ln(2)	350.3/352.1		1Al(10)	302.9/302.1		1Al(8)	303.5/303.9		2Al(3)	294.9/294.7
Re(2):	2Al(2)	255.9/256.0		1Al(1)	303.1/300.7		1Ln(1)	304.1/303.9		1Ln(2)	319.2/322.1
	2Al(12)	260.2/260.2		1Al(9)	309.2/311.2		2Al(5)	312.3/313.7		2Al(5)	358.2/357.8
	2Al(8)	264.5/264.1		1Ln(1)	324.6/324.4		2Al(3)	343.7/344.0		1Al(11)	390.0/392.7
	2Al(3)	269.6/269.8		1Al(9)	328.4/329.6				Al(12):	2Re(2)	260.2/260.2
	2Al(9)	273.0/273.1		1Al(7)	343.7/344.0					2Al(2)	263.0/262.5
	2Ln(1)	349.7/350.2								2Al(8)	271.0/273.9
										2Al(3)	283.6/282.4
										2Al(9)	306.8/305.8
										2Ln(1)	323.3/325.4
										1Al(12)	382.4/388.3

[a] For the calculation of these distances the lattice constants obtained from the Guinier powder patterns were used. Standard deviations are equal to or less than 0.5 pm (environments of the Lu atoms), 0.4 pm (Re atoms), and 1.0 pm (Al−Al distances) for $LuRe_2Al_{10}$ and 1.0 pm (Yb), 0.7 pm (Re), and 1.7 pm (Al−Al) for $YbRe_2Al_{10}$, respectively. All distances shorter than 400 pm are listed. They correspond to the coordination polyhedra shown in Figure 3 with the large Al(4)−Al(4) distance as the only exception.

ments the ideal occupancy values were resumed. The final difference Fourier synthesis revealed as highest and lowest values +5.3 and −2.7 e/Å^3. The highest value could correspond to an occupancy of ca. 30% with oxygen atoms; however, this site is too close (149 pm) to the fully occupied Al(3) position, and therefore there is no reason to consider this location as an atomic position. Subsequently the positional parameters of $LuRe_2Al_{10}$ were standardized using the program STRUCTURE TIDY.[10] The atomic parameters are given in Table 3, the anisotropic displacement parameters are given in a table of the Supporting Information, and the interatomic distances are listed in Table 4.

Structure Refinements of $YbRe_2Al_{10}$ and $NdRe_2Al_{10}$

In addition to the structure determination of $LuRe_2Al_{10}$ we refined this structure also from single-crystal X-ray data of the isotypic ytterbium compound. The structure of the new compound $NdRe_2Al_{10}$ was recognized to be isotypic with $CaCr_2Al_{10}$. Both structures were refined from four-circle diffractometer data using the same experimental conditions and the same computer programs as described above for $LuRe_2Al_{10}$.

Again, the occupancy parameters of both structures were refined together with anisotropic displacement parameters for all atoms (with the exception of one rhenium position) as described above. The X-ray data of $YbRe_2Al_{10}$ were of a lower quality than those of $LuRe_2Al_{10}$. Therefore, the occupancy parameters of the ytterbium compound showed greater deviations from the ideal values; they varied between 90(4)% and 111(5)% for the Al(6) and Al(12) positions, respectively. Nevertheless, because of the relatively large standard deviations, we assumed the ideal occupancy values in the final refinement cycles of this structure, especially also because the analogous refinement for the isotypic lutetium compound had shown practically full occupancy of all aluminum positions.

This was somewhat different for $NdRe_2Al_{10}$, where an occupancy parameter of 114(2)% was found for the Al(3) position. This position has a coordination which is similar to that of the rhenium atoms.[5] We therefore refined the Al(3) position with mixed occupancy. This refinement led to an Al:Re ratio of 0.960(4):0.040(4). However, the displacement

(10) Gelato, L. M.; Parthé, E. *J. Appl. Crystallogr.* **1987**, *20*, 139.

Table 5. Interatomic Distances of $NdRe_2Al_{10}$[a]

Nd(1):	4Al(2)	318.2(3)	Re:	2Al(4)	257.2(1)	Al(2):	1Al(1)	262.6(4)	Al(4):	2Re	257.2(1)
	4Al(1)	321.2(3)		1Al(3)	259.4(5)		2Al(3)	263.3(3)		2Al(3)	273.1(3)
	4Al(2)	329.3(3)		1Al(3)	260.4(4)		2Re	265.5(1)		2Al(5)	283.9(2)
	4Al(3)	332.0(3)		2Al(2)	265.5(1)		2Al(2)	275.2(4)		2Al(1)	286.3(3)
	4Re	361.7(1)		2Al(5)	275.2(1)		2Al(5)	295.5(3)		2Al(4)	291.9(4)
Nd(2):	4Al(5)	323.2(2)		2Al(1)	276.8(2)		1Al(1)	313.3(4)		2Nd(2)	330.9(2)
	8Al(4)	330.9(2)		1Nd(2)	337.9(1)		1Nd(1)	318.2(3)	Al(5):	1Al(5)	268.4(5)
	4Re	337.9(1)		1Nd(1)	361.7(1)		1Nd(1)	329.3(3)		2Re	275.2(1)
	4Al(3)	361.8(3)	Al(1):	1Al(2)	262.6(4)	Al(3):	1Re	259.4(4)		2Al(4)	283.9(2)
				1Al(1)	275.2(5)		1Re	260.4(5)		2Al(3)	284.7(2)
				2Re	276.8(2)		2Al(2)	263.3(3)		2Al(2)	295.5(3)
				2Al(3)	280.0(3)		2Al(4)	273.1(3)		2Al(1)	311.2(3)
				2Al(4)	286.3(3)		2Al(1)	280.0(3)		1Nd(2)	323.2(2)
				2Al(5)	311.2(3)		2Al(5)	284.7(2)		2Al(1)	333.0(3)
				1Al(2)	313.3(4)		1Nd(1)	332.0(3)			
				1Nd(1)	321.2(3)		1Nd(2)	361.8(3)			
				2Al(5)	333.0(3)						

[a] These distances were calculated with the lattice constants obtained from the Guinier powder patterns. All distances shorter than 385 pm are listed.

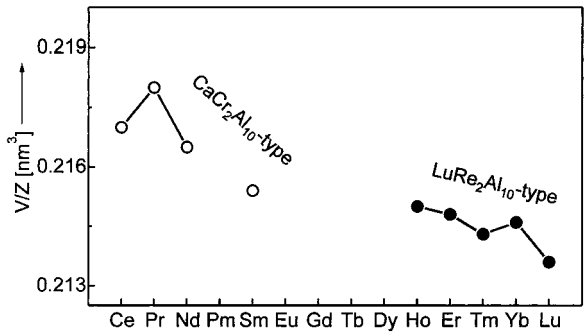

Figure 1. Cell volumes per formula unit of the rare earth rhenium aluminides $LnRe_2Al_{10}$ with $CaCr_2Al_{10}$- and $LuRe_2Al_{10}$-type structure.

parameters for this position, refined together with the occupancy parameter, were rather high ($B_{eq} = 0.85(7) \times 10^{-4}$ pm^2), thus compensating for the seemingly higher scattering power of this position. Furthermore, the structure refinements of the isotypic compounds $CeRe_2Al_{10}$ and $SmRe_2Al_{10}$ had not shown any larger scattering power for the Al(3) position.[5] Hence, in the final refinement cycles we assumed the ideal occupancy parameters also for this compound. Further details and results are summarized in Tables 2−5 and in the Supporting Information.

Discussion

In Figure 1 we have plotted the cell volumes per formula unit *V*/*Z* of the new rare earth rhenium aluminides, whose structure we have determined for the lutetium compound. We have found this structure type for the heavy late lanthanoids, while the light early lanthanoids, including the new compound $NdRe_2Al_{10}$, adopt a structure first reported for $CaCr_2Al_{10}$.[5,6] The cell volume of $CeRe_2Al_{10}$ is somewhat smaller than that of $PrRe_2Al_{10}$, and this has been ascribed to a mixed or intermediate +III/+IV valence of the cerium atoms.[5] Similarly, the cell volume found here for $YbRe_2Al_{10}$ deviates from the smooth function of the lanthanoid contraction. It is somewhat larger than that of $TmRe_2Al_{10}$, indicating a mixed or intermediate +II/+III valence for the ytterbium atoms. A much larger cell volume would be expected for $YbRe_2Al_{10}$ if the ytterbium atoms were purely divalent.

The structure of the $CaCr_2Al_{10}$-type lanthanoid rhenium aluminides has been discussed recently.[5] Therefore, we will focus our attention on the new structure found for the corresponding compounds of the late lanthanoids. A stereoplot of this structure with $LuRe_2Al_{10}$ as a representative is shown in Figure 2. As is usually observed for intermetallic compounds, all atoms have high coordination numbers (CN). The two different lutetium positions have very similar coordination polyhedra (Figure 3) with four rhenium and 16 aluminum neighbors yielding CN 20. These coordination polyhedra are very similar to the one found for the ytterbium atoms in $YbFe_2Al_{10}$.[7] They are also like those (again with four Re and 16 Al atoms) found in the $CaCr_2Al_{10}$-type structure of the compounds $LnRe_2Al_{10}$ with the early lanthanoids (Ln = Ce−Nd, Sm). This is somewhat surprising, since the early lanthanoid atoms are considerably larger than the late ones, and the fact that the structures of the compounds of the early and the late lanthanoids are frequently different can usually be rationalized by the different CNs of these atoms. The Lu−Al distances cover the differing ranges between 304.1 and 350.0 pm for the Lu(1) atoms, and between 302.5 and 390.7 pm for the Lu(2) atoms. The average Lu−Al distances, however, are very similar with 327.7 and 327.6 pm, respectively. They are shorter than the (average) Lu−Re distances of 344.1 and 350.3 pm. Since the metallic radius of aluminum (143.2 pm) is larger than that of rhenium (137.5 pm) this indicates that the Lu−Al bonding is stronger than the Lu−Re bonding. (The radii 143.2 pm (Al) and 137.5 pm (Re) (for CN 12) can readily be calculated from the lattice constants of the element structures. They are identical with those given by Teatum, Gschneidner, and Waber.[11]) The analogous situation is encountered in the coordination polyhedra of the two neodymium positions of $NdRe_2Al_{10}$ (Table 5).

The two different rhenium atoms in $LuRe_2Al_{10}$ and $YbRe_2Al_{10}$ as well as the rhenium atoms in the $CaCr_2Al_{10}$-type structure of $NdRe_2Al_{10}$ have nearly the same coordination: an icosahedron formed by 10 aluminum atoms and two rare earth atoms. The latter are situated on opposite sides of the icosahedra. The average Re−Al distances are nearly the same with 265.3 (265.6), 264.6 (264.6), and 266.9 pm for the Re(1) and Re(2) atoms of $LuRe_2Al_{10}$ ($YbRe_2Al_{10}$) and the one Re position of $NdRe_2Al_{10}$, respectively.

The 12 different aluminum atoms of $LuRe_2Al_{10}$ have between 12 and 14 neighbors. The polyhedra with CN 12—the coordination of the Al(1), Al(2), and Al(4) atoms—may all be considered as bicapped pentagonal antiprisms, i.e., as distorted icosahedra. The Al(6), Al(8), Al(10), and Al(12) atoms have CN 13. These coordination polyhedra are drawn in such a way in Figure 3 that their similarities can more easily be recognized. The

(11) Teatum, E.; Gschneidner, K.; Waber, J. *LA-2345*; U.S. Department of Commerce: Washington, DC, 1960. See: Pearson, W. B. *The Crystal Chemistry and Physics of Metals and Alloys*; Wiley: New York, 1972.

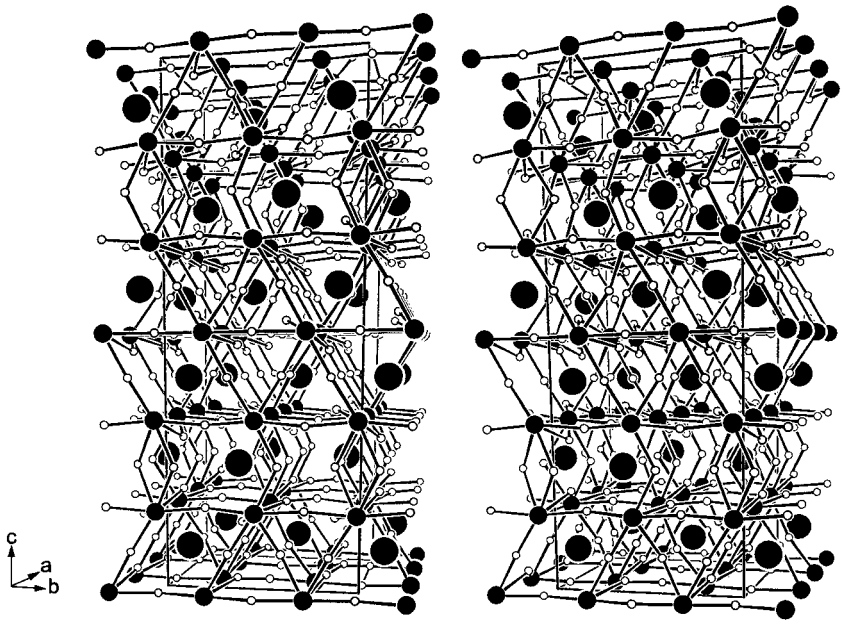

Figure 2. Stereoplot of the structure of $LuRe_2Al_{10}$ emphasizing the Re−Al bonding. The lutetium and rhenium atoms are represented by large and small filled circles, respectively, throughout the paper.

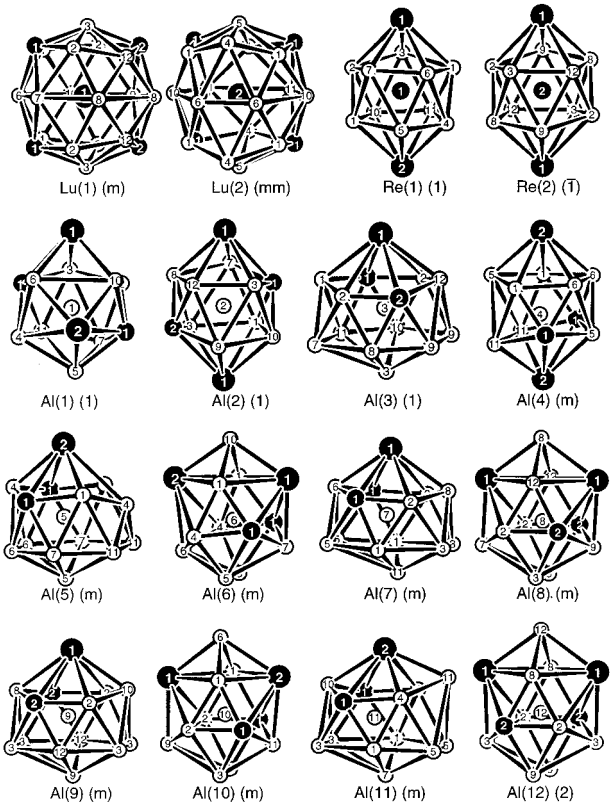

Figure 3. Coordination polyhedra in the structure of $LuRe_2Al_{10}$. The site symmetries of the central atoms are indicated in parentheses.

coordination polyhedra of the Al(3), Al(5), Al(7), Al(9), and Al(11) atoms with CN 14 may all be regarded as bicapped hexagonal antiprisms. It is remarkable that all of these coordination polyhedra have practically only triangular faces. In contrast, the $La_4Mo_7Al_{51}$-type structure,[12] with a composition similar to that of $LuRe_2Al_{10}$, has eight different aluminum positions, where all coordination polyhedra of the aluminum atoms have at least some almost rectangular faces. Most of the coordination polyhedra of the aluminum atoms in $La_4Mo_7Al_{51}$ are bicapped pentagonal or hexagonal prisms (in contrast to the antiprisms in $LuRe_2Al_{10}$). All coordination polyhedra of the aluminum atoms in $LuRe_2Al_{10}$ contain three or four heteroatoms of which one or two are lutetium atoms and two are always rhenium atoms. The average Al−Al distances reflect the different CNs of the aluminum atoms. For $LuRe_2Al_{10}$ they cover the range from 273.7 pm (Al(2)) to 281.0 pm (Al(1)) for those aluminum atoms with CN 12, from 291.0 pm (Al(10)) to 292.4 pm (Al(12)) for the aluminum atoms with CN 13, and from 298.3 pm (Al(3)) to 304.8 pm (Al(11)) for the aluminum atoms with CN 14. The corresponding ranges in the ytterbium compound are very similar: from 273.7 to 281.3 pm, from 291.5 to 293.1 pm, and from 298.4 to 305.3 pm, respectively. The Al−Al distances in $NdRe_2Al_{10}$ have similar ranges. The Al(2), Al(3), and Al(4) atoms with CN 12 have average Al−Al distances between 275.3 pm (Al(3)) and 283.8 pm (Al(4)); and the Al(1) and Al(5) atoms with CN 14 have average Al−Al distances of 297.5 and 298.6 pm, respectively.

The refinement of the occupancy parameters of $LuRe_2Al_{10}$, $YbRe_2Al_{10}$, and $NdRe_2Al_{10}$ showed that all atomic positions have ideal occupancies within four standard deviations. The only exception is the Al(3) position of $NdRe_2Al_{10}$ with an occupancy value of 114(2)%, as already discussed above. On close inspection, however, one may notice that almost all aluminum positions of the three structures have occupancy values of slightly less than 100%, while the rare earth and rhenium positions have slightly higher occupancy values than the aluminum positions (Table 3). The average occupancy value for the rare earth and rhenium positions is 99.6%, whereas for the aluminum positions the average is 97.9%. This systematic difference has led us to look at the occupancy values also for the structure refinements of other aluminum-rich compounds, which we have reported in recent years. Indeed, there is overwhelming evidence that the average aluminum positions of these compounds have smaller occupancy factors than the rare earth and transition metal positions. The results of this small survey are summarized in Table 6. In preparing this table we have included all of our structure refinements of recent years, where the occupancy values were available. Occasionally one

(12) Thiede, V. M. T.; Jeitschko, W. *J. Solid State Chem.* **1999**, *143*, 198.

Table 6. Occupancy Values Found during Structure Refinements of Intermetallic Compounds with High Aluminum Content[a]

	rare earth and transition metal atoms			aluminum atoms			
compd	no. of positions	range of occup (%)	av occup (%)	no. of positions	range of occup (%)	av occup (%)	ref
$LuRe_2Al_{10}$	4	98.9−100.7	99.9	12	96−103	99.1	this work
$YbRe_2Al_{10}$	4	98.9−100.0	99.7	12	90−111	96.5	this work
$NdRe_2Al_{10}$	3	98.8−100.0	99.1	5	94−114	98.6	this work
$Gd_{7.23}Re_{12}Al_{61.70}$	2	99.7, 100.1	99.9	5	97.8−102.7	99.5	2
$Dy_{7.50}Re_{12}Al_{61.17}$	2	99.7, 100.0	99.9	5	95.7−103.8	99.5	2
$Lu_{7.61}Re_{12}Al_{61.02}$	2	99.8, 100.0	99.9	5	93.9−101.8	97.5	2
$Y_{7.28}Re_{12}Al_{61.38}$	2	99.8, 100.0	99.9	5	96.7−99.3	98.2	1
$Ho_{7.32}Re_{12}Al_{61.48}$	2	99.5, 100.0	99.8	5	94.7−101.9	96.8	1
$TbMn_2Al_{10}$	3	100	100	5	89−100	96.2	5
$CeRe_2Al_{10}$	3	100	100	5	93.6−97.4	95.1	5
$SmRe_2Al_{10}$	3	100	100	5	82.8−95.8	91.6	5
$YbFe_2Al_{10}$	2	99.8, 99.9	99.9	5	96.6−100.2	98.6	7, 18
$SmFe_2Al_{10}$	2	99.7, 99.9	99.8	5	95.7−101.2	97.9	8, 19
$LaOs_2Al_{10}$	2	99.9, 101.1	100.5	5	92.6−102.2	97.6	8, 20
$La_{3.66}Mo_7Al_{50.26}$	3	99.5−101.4	100.2	8	94.9−100.5	98.5	12, 20
Re_4Al_{11}	2	100.4, 100.7	100.6	6	96−103	99.5	13
$ReAl_6$	1	100.7	100.7	3	96.4−98.6	97.6	13
$CeTi_2Al_{20}$	2	99.4, 103.8	101.6	3	97.7−99.2	98.4	14
$CeMo_2Al_{20}$	2	100, 100.3	100.2	3	99.2−100.4	99.7	14
$Dy_6Ti_4Al_{43}$	3	98.7−100.7	99.8	7	98.0−100.3	98.9	15
$EuTa_2Al_{20}$	2	100.3, 100.4	100.4	2	95.6, 96.3	96.0	16
$Ca_6W_4Al_{43}$	3	99.8−100.3	100.0	7	97.9−103.3	99.6	16
$EuCo_2Al_9$	2	99.2, 99.9	99.6	2	98.0, 99.5	98.8	17, 20
		weighted av: 100.0			weighted av: 97.9		

[a] For the respective atomic sites (rare earth/transition metal atoms and aluminum atoms) the number of "fully occupied" sites considered, the range of occupancy values found, and the average occupancy values are listed.

or the other atomic position was excluded from this summary, because it could not possibly be fully occupied for steric reasons, or because very unusual occupancy values could only be rationalized by mixed (e.g., T/Al) occupancies. It can be seen from Table 6 that in all structure refinements the rare earth and transition metal atoms have slightly higher occupancy values than the aluminum atoms. The weighted average values (In weighing we considered only the number of the atomic positions, not the standard deviations of the occupancy values.) are 100.0% for the rare earth and transition metal positions (Ln/T) and 97.9% for the aluminum positions. Since (as usual) the absolute scale factors of the X-ray intensities are not known, only the relative (Ln/T vs Al) occupancy values have significance. Hence, one could possibly assume some vacancies for the Ln/T as well as for the aluminum sites.

In discussing the lower occupancy values for the aluminum sites one may consider several rationalizations. For one, one naively could accept these aluminum defects for real, i.e., about 2−3% of the average aluminum positions may really not be occupied. This seems unlikely to us, because these compounds were all obtained from samples containing an excess of aluminum and these samples had been equilibrated at relatively low annealing temperatures. Furthermore, such relatively large amounts of systematic defects are unheard of for intermetallics. One may also consider the possibility that the theoretical scattering factor for the free (isolated) aluminum atom may not be entirely correct. This is difficult for us to check. One may also argue that the aluminum atoms are more or less the most electropositive components in most of the considered compounds, and for that reason they may have transferred some portion of their valance electrons (and hence their scattering power) to the other components of the compounds. This rationalization is plausible; however, one also has to consider that the aluminum content of the compounds listed in Table 6 is very high, and the number of atoms, which possibly could accept this partial electron transfer, is small. For that reason this effect cannot be large for the average aluminum atom. Also, there are examples, like $CeTi_2Al_{20}$,[14] $CeMo_2Al_{20}$,[14] $Dy_6Ti_4Al_{43}$,[15] and $Ca_6W_4Al_{43}$,[16] where aluminum is not the most electropositive component (the corresponding electronegativity values given by Pauling[21] are Ca, 1.0; Ce, 1.1; Dy, 1.2; Ti, 1.4; Mo, 1.8; W, 1.7; and Al, 1.5). Nevertheless, it seems likely to us that the theoretical scattering curve for the free aluminum atom may not very well fit the electron distribution of the aluminum atoms in the solid. Finally, one should keep in mind that a defect of on the average of 2.1% amounts to only 0.27 electron per aluminum atom.

In Figure 4 we show projections along the three translation periods of the orthorhombic structure of $LuRe_2Al_{10}$ together with corresponding projections of the orthorhombic $YbFe_2Al_{10}$-type and tetragonal $ThMn_{12}$-type structures. It can be seen that these structures are closely related. Nevertheless, the structures are difficult to visualize. For that reason we have enframed certain atoms with the rectangles **C** and **D** and with the circles **E** and **F** of the $LuRe_2Al_{10}$ structure in Figure 4 and show these cutouts in projections at an angle in Figure 5, emphasizing the enviroments of the Lu(1) and Lu(2) atoms. The structure of $YbFe_2Al_{10}$ has already been described as a combined substitution and stacking variant of the $ThMn_{12}$-type structure.[7] At best this can be guessed from the projections of the two structures along

(13) Niemann, S.; Jeitschko, W. *Z. Naturforsch.* **1993**, *48b*, 1767.
(14) Niemann, S.; Jeitschko, W. *J. Solid State Chem.* **1995**, *114*, 337.
(15) Niemann, S.; Jeitschko, W. *J. Solid State Chem.* **1995**, *116*, 131.
(16) Thiede, V. M. T.; Jeitschko, W.; Niemann, S.; Ebel, Th. *J. Alloys Compd.* **1998**, *267*, 23.
(17) Thiede, V. M. T.; Jeitschko, W. *Z. Kristallogr.—New Cryst. Struct.* **1998**, *214*, 149.
(18) Niemann, S. Strukturchemische Untersuchungen an binären und ternären intermetallischen Verbindungen der Übergangsmetalle mit hohem Aluminiumgehalt. Dr. rer. nat. thesis, Universität Münster, 1994.
(19) Thiede, V. M. T. Diplomarbeit, Universität Münster, 1994.
(20) Thiede, V. M. T. Darstellung, Struktur und Eigenschaften binärer und ternärer intermetallischer Verbindungen mit hohem Aluminiumgehalt. Dr. rer. nat. thesis, Universität Münster, 1997.
(21) Pauling, L. *The Chemical Bond*; Cornell University Press: Ithaca, NY, 1968.

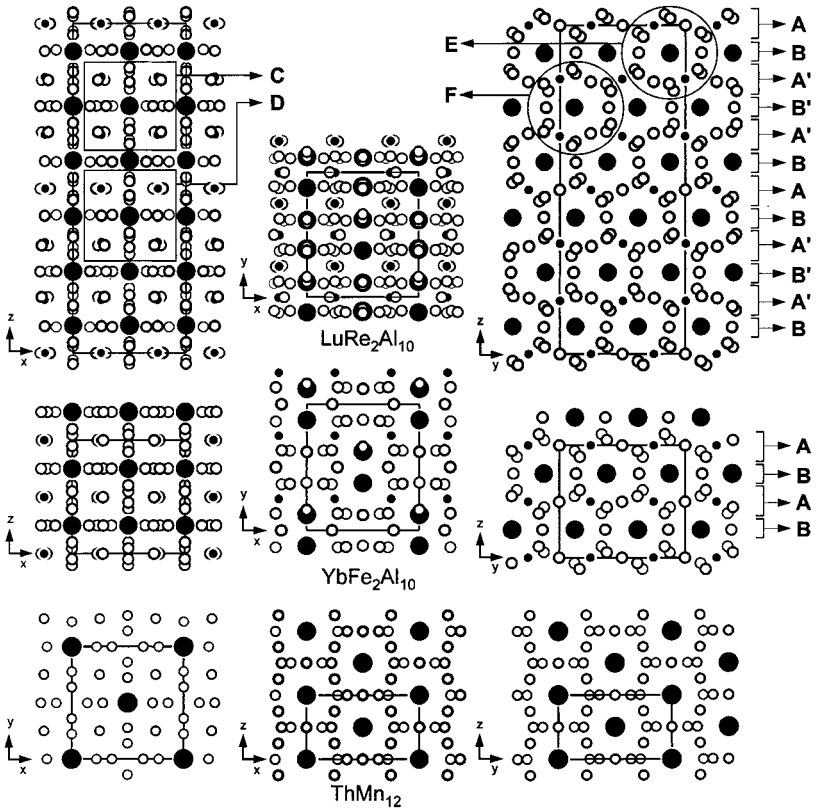

Figure 4. Crystal structure of $LuRe_2Al_{10}$ (space group *Cmcm*) as compared to the structures of $YbFe_2Al_{10}$ (*Cmcm*) and $ThMn_{12}$ (*I*4/*mmm*). The outlined rectangular prisms **C** and **D**, the tubes **E** and **F**, and the layers **A**, **B**, **A′**, and **B′** are shown in projections perpendicular to the present ones in Figure 5.

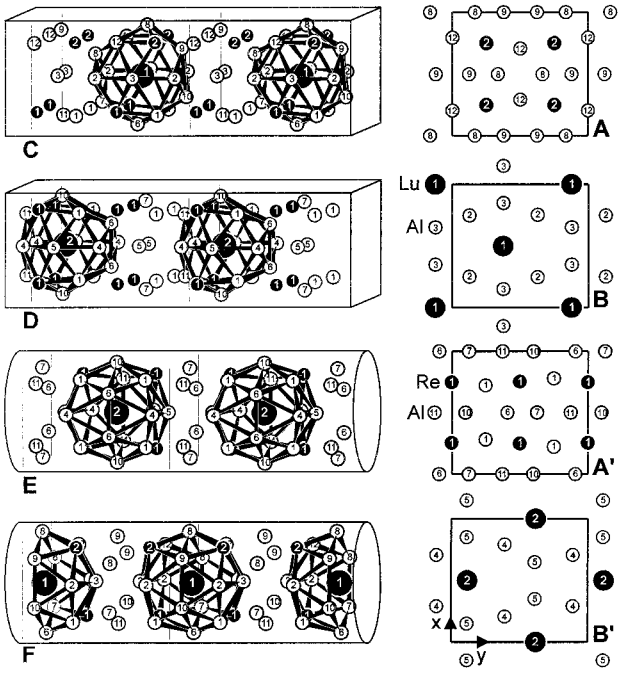

Figure 5. The prisms **C** and **D**, the tubes **E** and **F**, and the layers **A**, **B**, **A′**, and **B′** of Figure 4 shown from different points of view. The numbers within the atom symbols correspond to the atom designations of $LuRe_2Al_{10}$. The translation periods within the prisms **C** and **D** and within the tubes **E** and **F** are indicated by thin vertical lines.

the *z* ($YbFe_2Al_{10}$) and *y* axes ($ThMn_{12}$), respectively, in the middle part of Figure 4. The reader is referred to the figures of this earlier publication,[7] where this is illustrated in more detail. Here we focus our attention on the relationship between the structures of $LuRe_2Al_{10}$ and $YbFe_2Al_{10}$. These turned out to be stacking variants of each other. This is demonstrated with the atomic layers **A** and **B**, which are shown from the side in Figure 4. The four uppermost layers **A**, **B**, **A′**, and **B′** on the right-hand part of this figure are shown in views perpendicular to the layers in Figure 5. In both the $LuRe_2Al_{10}$ and the $YbFe_2Al_{10}$ structures layers of type **A** alternate with layers of type **B**. The complete stacking sequences of the layers for both structures are available in a figure of the Supporting Information.

Besides aluminum atoms the layers **A** contain the transition metal atoms (T) in the ratio T:Al = 1:3. These layers are hexagonally close packed. Disregarding the slight puckering of these layers, the arrangement of the transition metal and aluminum atoms within the layers corresponds to the rectangular mesh designated *R* by Beck and known from the three-dimensionally close-packed structure of $TiAl_3$.[22] One mesh of type **A** contains two formula units TAl_3. The layers of type **B** are less densely packed. One mesh of type **B** contains one formula unit $LnAl_4$. Thus, the compounds may also be designated with the formula $LnAl_4 \cdot T_2Al_6$. Similarly, the compounds $Ln_4T_9Al_{24}$ with T = Pd and Pt crystallize with a new structure type,[23] which contains two kinds of layers with the compositions Ln_2Al_3 and T_3Al_6 in the ratio 2:3 (i.e., $Ln_4T_9Al_{24} = 2Ln_2Al_3 \cdot 3T_3Al_6$). In this structure the layers with the composition T_3Al_6 are again close packed with an arrangement as it is known from the structures of the transition metal disilicides.[24,25]

The $CaCr_2Al_{10}$-type structure refined here for the new compound $NdRe_2Al_{10}$ has already been reported for $CeRe_2Al_{10}$,

(22) Beck, P. A. Close-Packed Ordered Alloys. In *Advances in X-Ray Analysis*; Barrett, C. S., Newkirk, J. B., Mallett, G. R., Eds.; Plenum Press: New York, 1969; Vol. 12, pp 1−22.
(23) Thiede, V. M. T.; Fehrmann, B.; Jeitschko, W. *Z Anorg. Allg. Chem.*, in press.
(24) Laves, F.; Wallbaum, H. J. *Z. Kristallogr.* **1939**, *101*, 78.
(25) Jeitschko, W. *Acta Crystallogr.* **1977**, *B33*, 2347 and references therein.

$PrRe_2Al_{10}$, and $SmRe_2Al_{10}$ and the homologous series $LnMn_2Al_{10}$.[5] This primitive tetragonal structure is a substitution variant of the body-centered tetragonal $ThMn_{12}$-type structure with a $2^{1/2}$ larger *a* axis, as can be seen by comparing the corresponding projections of Figures 4 and 6.

Acknowledgment. We thank U. Ch. Rodewald for competent data collections on the four-circle diffractometer as well as K. Wagner and H.-J. Göcke for the investigations at the scanning electron microscope. We are also grateful to Dr. G. Höfer (Heraeus Quarzschmelze) for a generous gift of silica tubes. This work was supported by the Deutsche Forschungsgemeinschaft, the Fonds der Chemischen Industrie, and the International Centre for Diffraction Data.

Supporting Information Available: Listings of crystallographic data and anisotropic displacement parameters for all atoms of $LuRe_2Al_{10}$, $YbRe_2Al_{10}$, and $NdRe_2Al_{10}$ and a figure with the layer sequences of the $LuRe_2Al_{10}$ and $YbFe_2Al_{10}$ structures. This material is available free of charge via the Internet at http://pubs.acs.org.

IC990073N

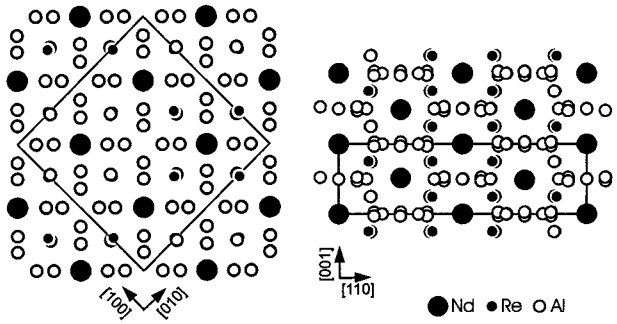

Figure 6. Crystal structure of $NdRe_2Al_{10}$ ($CaCr_2Al_{10}$-type) projected along directions corresponding to those used in Figure 4.